Pharmaceutical Research, Vol. 27, No. 2, February 2010 (© 2009)
DOI: 10.1007/s11095-009-9995-y

Research Paper

Rational Design of Multiple TB Antigens TB10.4 and TB10.4-Ag85B as Subunit Vaccine Candidates Against *Mycobacterium Tuberculosis*

Shuai Shi,[1] Lan Yu,[2] Dengyun Sun,[3] Jian Liu,[4] and Anthony J. Hickey[1,5]

Received July 9, 2009; accepted October 12, 2009; published online October 28, 2009

Purpose. Rational design of recombinant antigens TB10.4 and TB10.4-Ag85B as subunit vaccine candidates against *Mycobacterium tuberculosis*. The main purpose is to obtain a large quantity of soluble antigens.
Methods. Recombinant antigens were cloned in frame with the N-terminal thioredoxin and expressed in *E. coli*. The thioredoxin tag was removed by TEV protease. Nickel-affinity and size-exclusion chromatography were used to purify antigens to homogeneity. Antigen stability at different pH levels was studied by photon correlation spectrometry. Circular dichroism was used to probe antigen secondary structure and thermal stability.
Results. N-terminal thioredoxin fusion dramatically increased antigen solubility. Soluble TB10.4 and TB10.4-Ag85B were purified to homogeneity and obtained in milligram quantity. Co-expression of bacteria chaperons increased the yield of TB10.4-Ag85B. Soluble TB10.4 and TB10.4-Ag85B purified from the inclusion body showed a reversible structure change. However, Ag85B and soluble TB10.4-Ag85B showed a clear melting temperature, above which the secondary structure was lost dramatically.
Conclusion. Soluble TB10.4 and TB10.4-Ag85B were purified from the *E. coli* in significant quantities. The methods to purify and characterize these recombinant antigens were established, which paved the way for further vaccine development based on these antigens.

KEY WORDS: circular dichroism; *mycobacterium tuberculosis*; protein secondary structure; subunit vaccine; TB10.4-Ag85B.

INTRODUCTION

Tuberculosis (TB), caused by *Mycobacterium tuberculosis (MTB)* infection, is the leading cause of mortality in the world (1,2). Around 5% of the infected individuals develop pulmonary diseases in 2–5 years; the rest may develop the latent TB infection, and these individuals have about 5% lifetime chance of TB, reactivation (3). Bacillus Calmette-Guérin (BCG) is the only vaccine currently marked for TB (4). However, its prophylactic use has demonstrated varying levels of efficacy in distinct populations and different field trials (5,6). One explanation for this variability is thought to be the waning of protective efficacy of BCG after approximately 10–15 years (7). It has been reported that BCG revaccination does not confer additional protection and should not be recommended (8); hence, although effective against childhood TB (9,10), BCG has limited use against adult pulmonary disease. There is an urgent need to develop more effective vaccine either for prophylactic use or as a booster vaccine for BCG. Alternative vaccines include subunit vaccine (11), recombinant BCG (rBCG) (12,13), attenuated *MTB* (14,15) and non-replicating adenovirus carrying TB antigen (16).

Ag85 complex (Ag85A, B and C) is the most abundant protein secreted by *MTB* (17), which attracts considerable interests for new TB vaccine development. Ag85B has been shown to be among the most potent antigen species yet identified, which induces both humoral and cell-mediated immune responses in *MTB*-infected patients (18,19). Ag85B encapsulated in poly lactide-co-glycolide (PLGA) induced significant amount of IL-2 production in an *in vitro* antigen presentation assay (20). Together with ESAT-6, a TB subunit vaccine comprised of these two antigens induced high levels of protective immunity in mice and reached the level of BCG-induced protection (21). An rBCG vaccine expressing Ag85B (rBCG30) induced greater protective immunity against aerosol challenge with *MTB* than conventional BCG in a highly susceptible guinea model (13). TB10.4 is a protein belonging to the ESAT-6 protein family comprising ESAT-6, CFP-10, TB10.4, TB10.3, *etc.* (22,23). TB10.4 is strongly recognized by BCG-vaccinated donors and was even more strongly recognized in TB patients compared to ESAT-6 (24). Substitution TB10.4 for ESAT-6 allows the use of ESAT-6 as a diagnostic marker to distinguish *MTB*-infected individuals from healthy BCG-vaccinated individuals since ESAT-6 is only expressed in *MTB* but not in BCG (11). In light of this, a recombinant fusion of Ag85B and TB10.4 (Ag85B-TB10.4) was developed, which has been shown to induce strong protection against *MTB* comparable to BCG (11).

[1] Molecular Pharmaceutics, School of Pharmacy, University of North Carolina at Chapel Hill, Chapel Hill, North Carolina 27599-7360, USA.
[2] School of Pharmacy, Lanzhou University, Lan Zhou, Gan Su Province 730000, China.
[3] Intercollege Graduate Program in Cell and Developmental Biology, Pennsylvania State University, University Park, Pennsylvania, USA.
[4] Medicinal Chemistry and Natural Product, School of Pharmacy, University of North Carolina at Chapel Hill, Chapel Hill, North Carolina 27599-7360, USA.
[5] To whom correspondence should be addressed. (e-mail: ahick ey@unc.edu)

Although possible to purify native antigens from *MTB* cultures, it is much easier and safer to express them in *E. coli* as recombinant antigens (25). Moreover, molecular engineering can be employed to redesign antigens of interest and combine the advantages of different antigens (26). A similar strategy has been used to produce recombinant antigens for other vaccines, such as anthrax vaccine (27) and influenza vaccine (28). Although generally preferable to obtain recombinant antigens from the soluble fraction of *E. coli* culture, most antigens currently explored for TB subunit vaccine were frequently purified from the inclusion body as reported by several research groups (11,24,29,30). This is due to the tendency of incorrect protein folding and aggregation when expressed in the heterologous expression system such as *E. coli* (31,32).

Thioredoxin is a 12 KD protein involved in several cellular functions, such as sulfate metabolism, reduction of protein disulfides and as a cofactor for T7 DNA polymerase (33). It has a characteristic tertiary structure termed thioredoxin fold, which renders this protein highly stable and soluble (34,35). When fused N-terminally to other proteins, thioredoxin remarkably increased the solubility of the fusion protein, for example, mammalian cytokines and growth factors (36). Another advantage is that thioredoxin is localized on the cytoplasmic face of the adhesion zones between the outer and inner cell membranes (37). It can be exploited for rapid purification given that this property is retained by the fusion protein (36).

In the present study, solubility enhancement by N-terminal thioredoxin fusion was investigated in several recombinant antigens, such as TB10.4 and TB10.4-Ag85B. In order to study the effect of construct design on antigen folding, the solubility and yield of Trx-TB10.4-Ag85B was compared to that of Trx-Ag85B-TB10.4. A conformation comparison was made between TB10.4-Ag85B purified from the inclusion body and its soluble counterpart by circular dichroism (CD). CD was also extensively used to probe antigen secondary structure and thermal stability in this study.

MATERIALS AND METHODS

Constructs Design

Four constructs were designed as shown in Fig. 1a–d. Fig. 1a: Trx-TB10.4. TB10.4 was amplified from the H37Rv genome by the following primers: 5′-ATGGATCCATGTCG CAAATCATGTACAACTAC-3′ (F) and 5′-GTAGAATT CCTAGCCGCCCCATTTGGCGGCTTCGGCCGTGT-3′ (R). The PCR product was digested with BamH I and EcoR I and ligated into a customized pET32b vector, in which a TEV protease cleavage site was introduced between the $(His)_6$-tag and the multiple cloning sites. Fig. 1b: His-Ag85B-TB10.4. His-Ag85B was encoded in the pRSET-B vector (courtesy of Dr. Douglas Kernodle, Vanderbilt University). TB10.4 was amplified from the H37Rv genome by the following primers: 5′-ATGCATGGCGCCGGCATGTCGCAAATCATGTAC AACTACC-3′ (F) and 5′-GTAGAATTCCTAGCCGCCC CATTTGGCGGCTTCGGCCGTGT-3′ (R). The PCR product was digested with Nar I and EcoR I and ligated in frame with His-Ag85B to generate the fusion molecule His-Ag85B-TB10.4. Fig. 1c: Trx-Ag85B-TB10.4. Both 5′-TAAGG ATCCTTCTCCCGTCCGGGTCTGCCGGTC-3′ (F) and 5′-ATAGAATTCCTAGCCGCCCCATTTGGCGGCTTC-3′ (R) were used to amplify Ag85B-TB10.4 by using His-Ag85B-TB10.4 as the template. The PCR product was then introduced into the customized pET32b vector between BamH I and EcoR I restriction sites. Fig. 1d: Trx-TB10.4-Ag85B. TB10.4 was amplified by 5′-ATCGGATCCATGT CGCAAATCATGTACAAC-3′ (F) and 5′-GCCGCCC CATTTGGCGGCTTC-3′ (R). Ag85B was amplified by 5′-^{P}TTCTCCCGTCCGGGTCTGCCGGTC-3′ (F, with 5′ phosphate) and 5′- ATAGAATTCTCAGCCGGCGCCT AACGAACT-3′ (R). The two PCR fragments were ligated by T4 DNA ligase and re-amplified to obtain the fusion protein. The PCR product was then inserted into the customized pET32b vector between BamH I and EcoR I restriction sites.

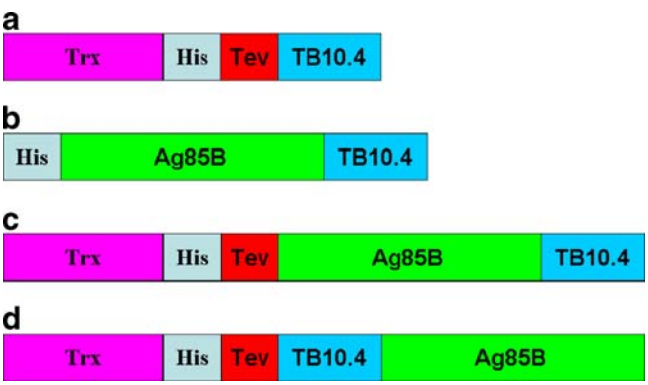

Fig. 1. Construct design for recombinant antigens. **a**, Trx-TB10.4 in customized pET32b vector; **b**, His-Ag85B-TB10.4 in pRSET-B vector; **c**, Trx-Ag85B-TB10.4 in customized pET32b vector; **d**, Trx - TB10.4-Ag85B in customized pET32b vector.

Expression of Recombinant Antigens

Recombinant Ag85B and Trx-TB10.4 were expressed in *E. coli BL21 (DE3)* strain (Stratagene). Typically, 1 L Luria-Bertani (LB) broth with 50 μg/ml carbenicillin was inoculated with 20 ml of an overnight culture and grown at 37°C until the OD600 reached 0.6–0.8. The culture was induced by addition of 100 μM isopropyl-β-thiogalactopyranoside (IPTG) and grown at 18°C overnight. Recombinant His-Ag85B-TB10.4, Trx-Ag85B-TB10.4 and Trx-TB10.4-Ag85B were expressed in *E. coli Origami B* strain (Novagen) either with or without a plasmid expressing chaperon GroEL /GroES. 50 μg/ml carbenicillin, 12.5 μg/ml tetracycline, 15 μg/ml kanamycin and 20 μg/ml chloramphenicol were supplemented into the medium. L-arabinose (1 mg/ml) and IPTG (100 μM) were used to induce chaperon and antigen expression, respectively, at 18°C overnight.

Antigen Purification from the Soluble Fraction

E.coli cells were pelleted, washed twice with phosphate buffered saline (PBS), re-suspended in PBS containing 1 mM phenylmethylsulphonyl fluoride (PMSF) and then probe-sonicated 3 times. The resulting preparation was centrifuged at 15,000 rpm for 30 min. The soluble fraction of the recombinant antigens resides in the supernatant, while inclusion body remains in the pellet. To purify soluble His-Ag85B, the supernatant was passed through a nickel column (Ni Sepharose™ 6 Fast Flow, Amersham Biosciences, Piscataway, NJ). The eluted proteins were further purified by a Superdex 75 column (Amersham Biosciences,

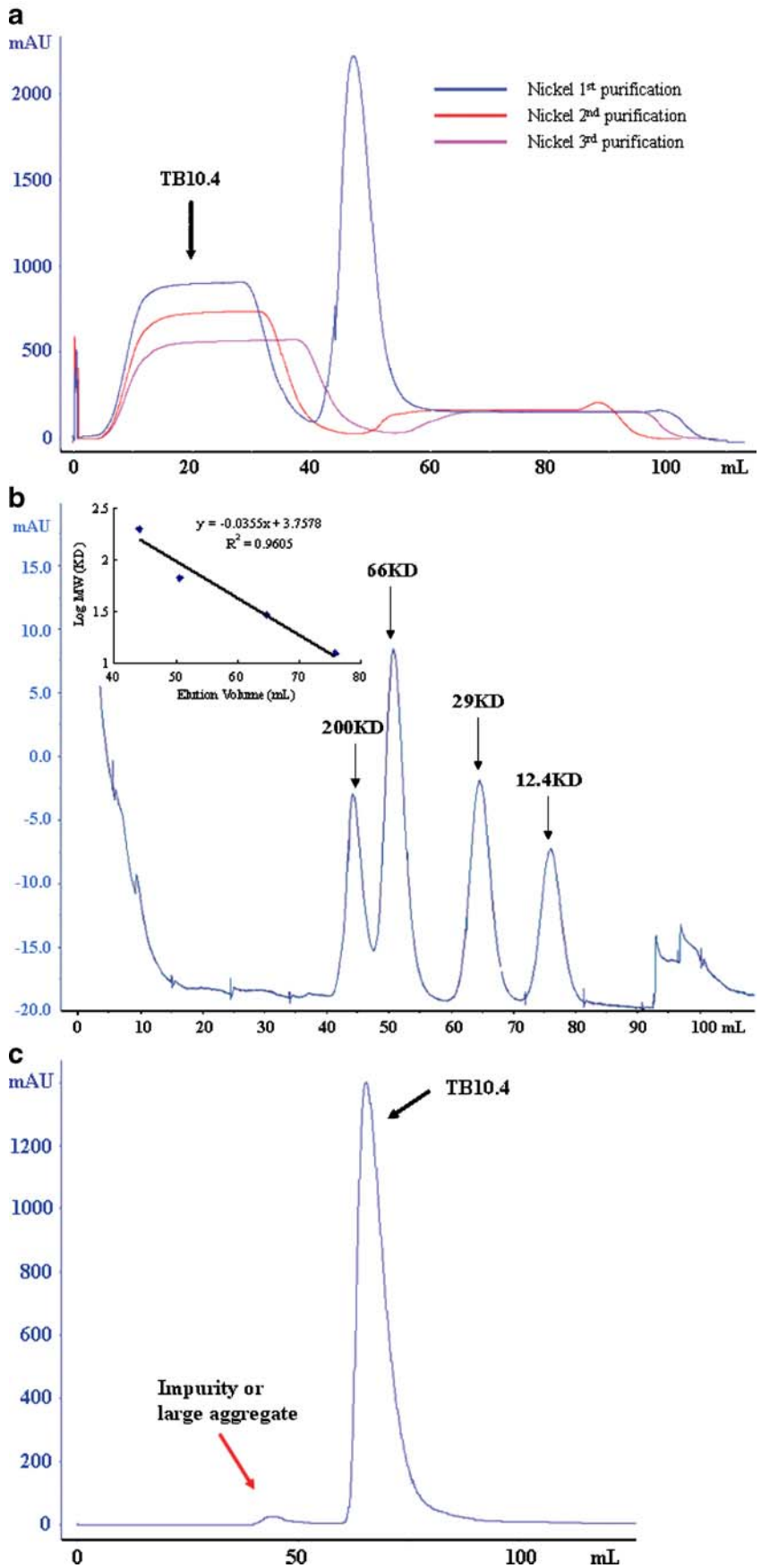
a
mAU
2000
1500
1000
500
0
Nickel 1st purification
Nickel 2nd purification
Nickel 3rd purification
TB10.4
0
20
40
60
80
100
mL
b
mAU
15.0
10.0
5.0
0.0
-5.0
-10.0
-15.0
-20.0
y = -0.0355x + 3.7578
R2 = 0.9605
Log MW (KD)
Elution Volume (mL)
66KD
29KD
200KD
12.4KD
0
10
20
30
40
50
60
70
80
90
100 mL
c
mAU
1200
1000
800
600
400
200
0
TB10.4
Impurity or
large aggregate
0
50
100
mL

◀ **Fig. 2.** TB10.4 purification by nickel-affinity and size-exclusion chromatography. **a**, chromatogram of TB10.4 purified by nickel-affinity column; **b**, calibration of Superdex 75 column with protein standards (cytochrome c: 12.4 KD; carbonic anhydrase: 29 KD; bovine serum albumin: 66 KD; β-amylase: 200 KD). The log-transformation of protein molecular weight was linearly correlated with the elution volume (inset, upper left corner); **c**, chromatogram of TB10.4 further purified by Superdex 75 column.

Piscataway, NJ) with 20 mM MOPS, 0.4 M sodium chloride, pH 7.0 as the eluting buffer at a flow rate of 1 ml/min. Soluble Trx-TB10.4, Trx-Ag85B-TB10.4 and Trx-TB10.4-Ag85B were purified on a nickel column first. Eluted proteins were dialyzed against Tris-HCl buffer (pH 7.4) to eliminate imidazole. Dialyzed proteins were treated with TEV protease (His-tagged) at a ratio of 25:1 (w/w) overnight at 4°C. The reaction mixture was spiked with 5 mM imidazole before loading onto the nickel column. Protein unbound to the nickel column was collected, and the same procedure was repeated two more times (Fig. 2a). Proteins were concentrated to 5 ml and further purified on a Superdex 75 column (for TB10.4) or Superdex 200 column (for TB10.4-Ag85B) eluted with 20 mM MOPS, 0.4 M sodium chloride, pH 7.0 as the eluting buffer at a flow rate of 1 ml/min.

Antigen Purification from the Inclusion Body

To purify antigen from the inclusion body, the pellet from 1 L culture was first washed with PBS three times. 30 ml of Tris-HCl buffer (pH 7.4) containing 8 M urea was then added to resolubilize the inclusion body at 4°C for 4 h followed by centrifugation at 15, 000 rpm for 1 h. The supernatant was passed through a 0.2 μm filter to eliminate any insoluble matters. 1 ml urea-resolubilized protein was then added dropwise into a beaker containing 50 ml Tris-HCl (pH 7.4) buffer with gentle mixing on ice. The diluted protein was passed through a 0.2 μm filter immediately after the dilution. Antigen in the filtrate was then purified by a combination of nickel-affinity and size-exclusion chromatography as describe above.

SDS-PAGE, Native-PAGE, Image Analysis and Antigen Concentration Determination

A precast 12% SDS-PAGE gel (Biorad, Hercules, CA) was used to determine the purity of the recombinant antigens. A precast 10% Tris-glycine native gel (Biorad, Hercules, CA) was used for native-PAGE. The gel was stained with Coomassie blue. The intensity of the bands in the gel was analyzed in ImageJ (http://rsbweb.nih.gov/ij/). The antigen concentration was determined by BCA™ protein assay kit (Thermo Scientific, Rockford, IL).

Effect of Buffer pH on Antigen Stability

Citrate-phosphate buffer covering the range from pH 3 to pH 8 was prepared to study antigen stability at different pH levels. Antigen stock in MOPS buffer (20 mM, pH7.0) was diluted 20 times into the citric-phosphate buffer with the corresponding pH. This dilution ensures that the pH of the citric-phosphate buffer was not changed significantly by the introduction of MOPS buffer. The diluted antigen solution has a concentration between 0.05 mg/ml and 0.1 mg/ml. The samples were left at room temperature for an appropriate time period as shown in Fig. 4. The size and distribution of antigen aggregates were measured by photon correlation spectrometry (PCS) employing the particle sizer (NICOMP particle sizing systems, Autodilute^{PAT} Model 370, Santa Babra, CA) in the NICOMP mode and repeated three times.

Multiple Sequence Alignment, Protein Structure Simulation and pI Prediction

Sequence alignment of ESAT-6 family members TB10.4, TB10.3, ESAT-6 and CFP-10 was carried out in ClustalW (http://align.genome.jp/). The 3D coordinates for Ag85B (PDB accession #: 1F0N) were downloaded from protein database bank (PDB) and reconstructed in PyMOL (http://pymol.sourceforge.net/). Since there is no crystal structure available for TB10.4, SWISS-MODEL (http://swissmodel.expasy.org/) was used to simulate the structure of TB10.4 based on sequence homology. The first approach mode identified CFP-10/ESAT-6 (PDB accession #: 1wa8) as the template for simulation. Simulated structure of TB10.4 was constructed in PyMOL. ProtParam (http://www.expasy.ch/cgi-bin/protparam) was used to predict the isoelectric points (pI) of the proteins listed in Table I .

Circular Dichroism (CD) to Study Antigen Secondary Structure and Thermal Stability

Applied Photophysics Pistar-180 circular dichroism was used for this study. Buffer exchange was first performed to keep antigens in the CD-compatible buffer (10 mM potassium phosphate buffer, pH 7.4). The final antigen concentration for

Table I. Characterization of Recombinant Antigens

Protein	AAs	MW (KD)	pI[a]	Solubility	Yield (mg/L)
Ag85B	318	34	5.24	S[b]	5
His-TB10.4	129	14	5.23	IB[c]	N/A
Trx-TB10.4	269	29	5.16	S	14
TB10.4	105	11.3	4.82	S	4
Trx-Ag85B-TB10.4	554	60	5.05	WS[d] + IB	N/A
Trx-TB10.4-Ag85B	554	60	5.05	S + IB	2.5
TB10.4-Ag85B	390	42	4.85	S	1
His-Ag85B-TB10.4	414	45	5.02	IB	N/A

a: isoelectric point (predicted by ProtParam, see Materials and Methods)
b: soluble; c: inclusion body; d: weekly soluble

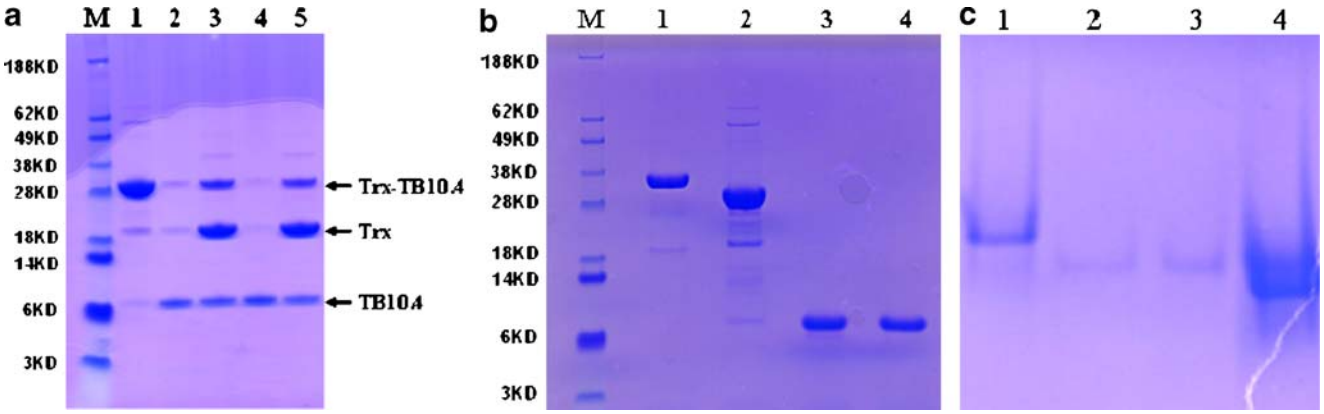

Fig. 3. SDS-PAGE and native-PAGE analysis of the recombinant antigens. **a**, SDS-PAGE analysis of Trx-TB10.4 and its digestion products. lane 1: Trx-TB10.4; lane 2: Trx-TB10.4 was treated with TEV protease and then passed through the nickel column. The flow-through was collected; lane 3: proteins bound to the column were eluted and collected; lane 4: duplicate of lane 2; lane 5: duplicate of lane 3; **b**, SDS-PAGE analysis of purified antigens. lane 1: Ag85B; lane 2: Trx-TB10.4; lane 3 and 4: TB10.4; **c**, native-PAGE analysis of purified antigens. lane 1: Ag85B; lane 2 and 3: TB10.4; lane 4: thioredoxin.

CD study ranges from 0.2 to 0.3 mg/ml. A full scan from 260 nm to 185 nm was first taken on each antigen at 20°C. The wavelength corresponding to the peak was selected to follow with temperature ramping from 20°C to 94°C (1°C/min). The selected wavelength was 220 nm for TB10.4, 216 nm for Ag85B and 218 nm for TB10.4-Ag85B. A full CD spectrum was also taken at 94°C, and then antigen samples were cooled to 20°C, at which point a full CD spectrum was recorded again. Blank spectrum (buffer only) was subtracted from all antigen CD spectrums. Best fit based on residual analysis was selected for curve fitting.

RESULTS

Production of Soluble Trx-TB10.4 and TB10.4

His-TB10.4 (encoded in pRSET-B vector) led to the exclusive formation of inclusion body in *E. coli* (data not shown). However, fusion of thioredoxin to the N-terminal of TB10.4 dramatically increased the solubility of Trx-TB10.4 (Fig. 1a) in comparing to His-TB10.4. Fig. 3a shows that the major band corresponding to Trx-TB10.4 (29KD, lane 1) was cleaved into two fragments corresponding to the thioredoxin and TB10.4, respectively. Surprisingly, TB10.4 released from the enzymatic cleavage was remarkably soluble and could be purified to homogeneity by a combination of chromatography (Fig. 2a and c). The sharp peak in Fig. 2c represents TB10.4, while the small preceding peak may represent protein impurities or large aggregate of TB10.4. Fig. 3b shows that TB10.4 can be purified to homogeneity (lanes 3 and 4).

TB10.4 Exists as an Oligomer

As shown in Fig. 2b, the Superdex 75 column was first calibrated with the protein standards. TB10.4 was eluted from the same column corresponding to a molecular weight of 27 KD. This apparent molecular weight is slightly greater than the calculated molecular weight of a TB10.4 dimer (22.6 KD). To further characterize this protein, TB10.4 was run on a native gel with Ag85B and thioredoxin for comparison (Fig. 3c). Both Ag85B (34 KD) and thioredoxin (19 KD) exist as monomer based on their elution volume from the Superdex 75 column (data not shown). Fig. 3c clearly shows that TB10.4 migrates faster than Ag85B yet

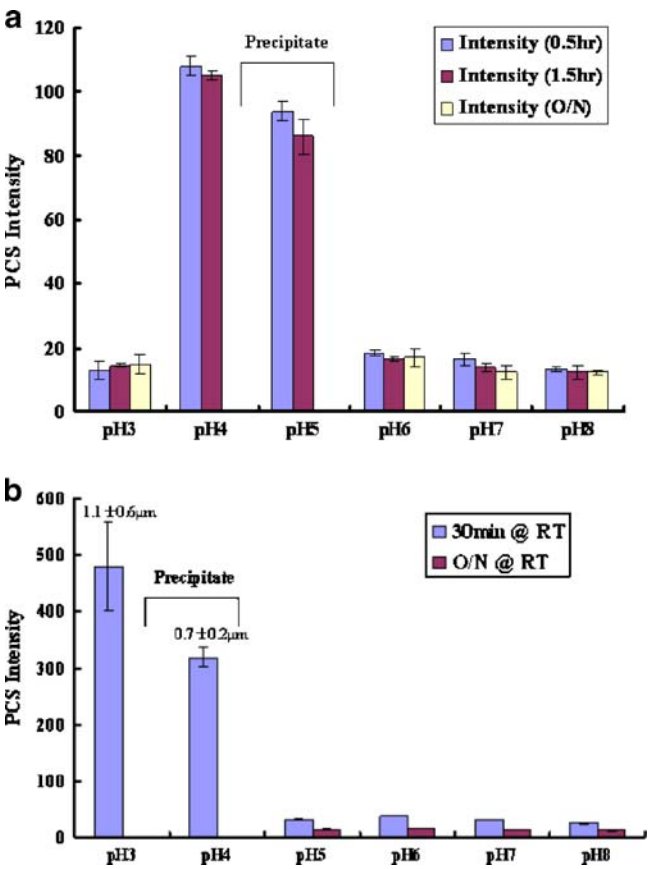

Fig. 4. Effect of buffer pH on antigen stability. **a**, buffer pH on Trx-TB10.4 stability; **b**, buffer pH on TB10.4 stability. For PCS intensity greater than 300, the size and distribution could be accurately calculated and labeled in the figure. For overnight incubation, the protein aggregates precipitate out from the solution, and no PCS intensity was recorded.

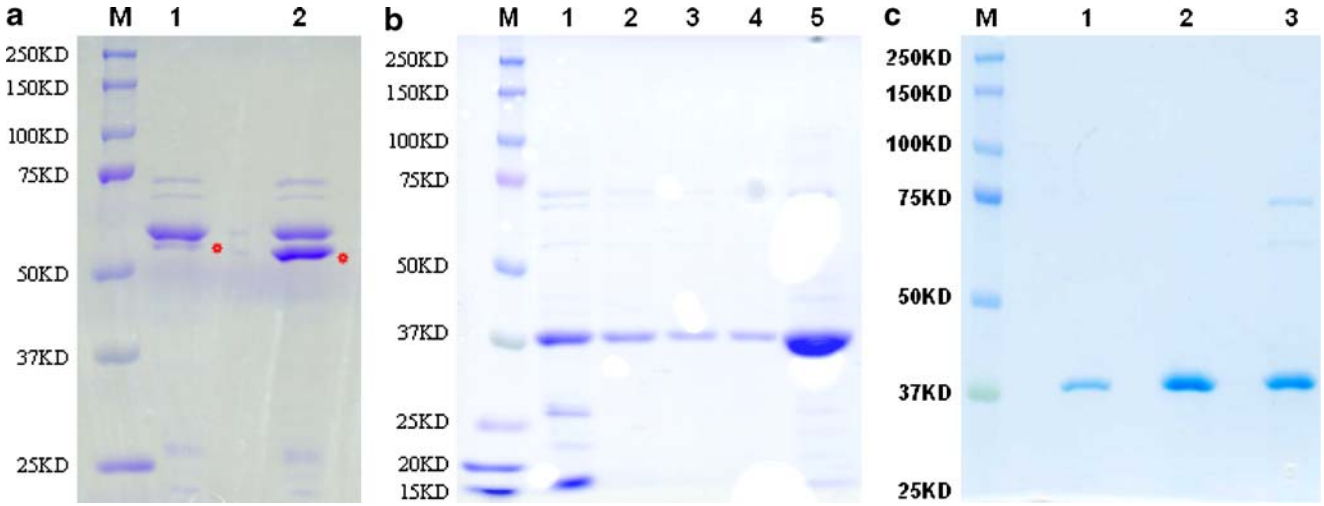

Fig. 5. SDS-PAGE analysis of recombinant antigens. **a**, SDS-PAGE analysis of nickel column purified antigens. lane 1: Trx-Ag85B-TB10.4 (indicated by asterisk); lane 2: Trx-TB10.4-Ag85B (indicated by asterisk); **b**, TB10.4-Ag85B released by TEV protease treatment was analyzed by SDS-PAGE. lane 1: Trx-TB10.4-Ag85B was treated with TEV protease overnight; lane 2: eluant of first pass through nickel column; lane 3: eluant of second pass through nickel column; lane 4: eluant of third pass through nickel column; lane 5: 10 times concentrate of the third eluant. **c**, TB10.4-Ag85B was further purified by GPC200 column. lane 1: 1 μg TB10.4-Ag85B; lane 2: 3 μg TB10.4-Ag85B; lane 3: 3 μg TB10.4-Ag85B prior to GPC200 purification.

slower than thioredoxin, which together with the chromatographic data suggest that TB10.4 exists as an oligomer.

Effect of pH on Trx-TB10.4 and TB10.4 Stability

As listed in Table I, all proteins studied are predicted to have the isoelectric point (pI) in a narrow acidic range (from 4.82 to 5.24). For Trx-TB10.4, significant protein aggregation was observed at pH 4 and pH 5, while no detectable aggregation was found at lower pH (<4) or higher pH (>5) monitored by photon correlation spectroscopy (Fig. 4a). The aggregation of Trx-TB10.4 starts immediately after diluting protein stock into appropriate buffer (pH 4 or 5). The aggregates may sustain in suspension for a couple of hours but precipitate out eventually. The aggregation of TB10.4 occurs at a lower pH range than that of Trx-TB10.4 as shown in Fig. 4b. This difference between the two proteins may be explained by the presence of thioredoxin in Trx-TB10.4, which is predicted to increase the pI of the fusion protein as shown in Table I.

Production of Soluble Trx-TB10.4-Ag85B and TB10.4-Ag85B

Initial expression of His-Ag85B-TB10.4 (Fig. 1b) leads to exclusive formation of inclusion body. Since the solubility of the recombinant antigen is a major concern, the fusion molecules were redesigned. In light of the success of Trx-TB10.4, two new molecules were constructed as shown in Fig. 1c (Trx-Ag85B-TB10.4) and Fig. 1d (Trx-TB10.4-Ag85B). Fig. 5a shows that the solubility of Trx-TB10.4-Ag85B was dramatically increased compared to Trx-Ag85B-TB10.4 (>10-fold increase analyzed in ImageJ). However, the solubility of Trx-Ag85B-TB10.4 is only slightly better than that of His-Ag85B-TB10.4. After TEV protease treatment, soluble TB10.4-Ag85B was released from the fusion molecule (Fig. 5b) and further purified to homogeneity (Fig. 5c).

Increasing the Yield of Trx-TB10.4-Ag85B by Co-expressing Chaperon Proteins

Compared to Trx-TB10.4, the yield of Trx-TB10.4-Ag85B was relatively low (Table I). This may be explained by 1) the latter protein being nearly twice the size of the former one, which consumes more energy to synthesize, or 2) the greater tendency for Trx-TB10.4-Ag85B to form inclusion body. Since the first explanation is an intrinsic property of the fusion protein, the improvement was focused on the second possibility. A chaperon protein GroEL/GroES was co-expressed with Trx-TB10.4-Ag85B, which increased the yield by at least 40% (Fig. 6). However, such improvement was minimal for Trx-Ag85B-TB10.4 (Fig. 6).

Purification of Trx-TB10.4-Ag85B from the Inclusion Body

Although thioredoxin fusion improves the folding of Trx-TB10.4-Ag85B significantly, a large quantity of mis-folded

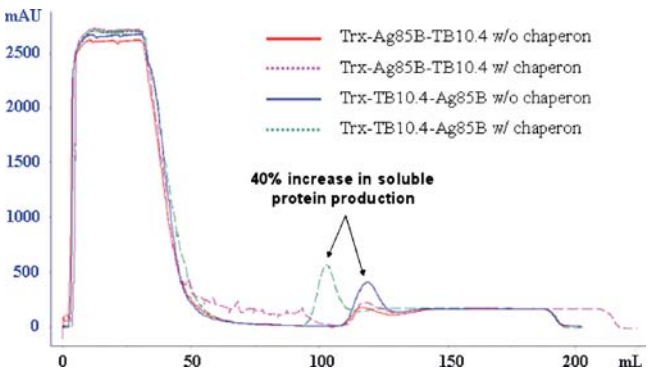

Fig. 6. Comparison of the yield of two recombinant antigens with or without the co-expression of chaperons. Chromatograms were shown of antigens purified by nickel-affinity chromatography.

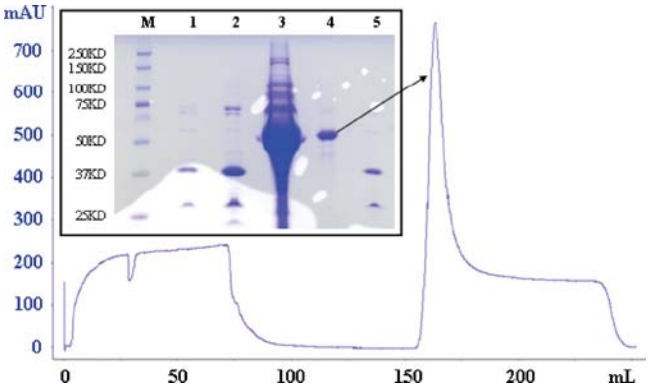

Fig. 7. Purification of Trx-TB10.4-Ag85B from inclusion body. Inset (upper left corner). lane 1: soluble Trx-TB10.4-Ag85B was treated with TEV protease; lane 2: same as lane 1 but different loading; lane 3: urea resolubilized Trx-TB10.4-Ag85B; lane 4: Trx-TB10.4-Ag85B in lane 3 was purified by nickel column; lane 5: purified Trx-TB10.4-Ag85B in lane 4 was cleaved by TEV protease into two fragments.

proteins was still found in the inclusion body (lane 3, Fig. 7). An effort was made to purify this protein from the inclusion body. The sharp peak in Fig. 7 represents Trx-TB10.4-Ag85B from the inclusion body, which was purified to homogeneity as demonstrated by SDS-PAGE (Fig. 7, lane 4). Trx-TB10.4-Ag85B purified from the inclusion body was also cleavable by TEV protease, evidenced by the appearance of two new polypeptides corresponding to TB10.4-Ag85B and thioredoxin, respectively (Fig. 7, lane 5).

Study Antigen Secondary Structure and Thermal Stability by Circular Dichroism

Fig. 8a shows the tertiary structure of Ag85B, comprising alpha-helixes, beta-sheets and linking loops. Based on sequence homology between TB10.4 and three other ESAT-6 family members (Fig. 8c), the structure of TB10.4 was simulated and constructed as shown in Fig. 8b. Significantly different from Ag85B, the structure of TB10.4 is dominated by alpha-helixes by prediction.

The CD spectrum of TB10.4 at 20°C (Fig. 9a, blue trace) again indicates that this antigen adopts an alpha-helix conformation. The results of thermal stability study suggest that TB10.4 lost its secondary structure gradually with temperature increase (Fig. 9aa). The CD spectrum recorded at 94°C (Fig. 9a, yellow trace) indicates a dramatic loss of secondary structure at high temperature. Surprisingly, TB10.4 almost fully regains its secondary structure when cooled to 20°C, suggesting a reversible structure change (Fig. 9a, pink and black traces as compared to the blue trace).

Remarkably different from TB10.4, Ag85B shows a clear melting temperature (Tm) at 73.7°C (Fig. 9bb). Moreover, Ag85B was not able to fully recover its secondary structure when cooled to 20°C (Fig. 9b, green and light blue traces as compared to the red trace), suggesting an irreversible structure change of this antigen.

The CD spectrum of soluble TB10.4-Ag85B (Fig. 9c) mimics that of Ag85B (Fig. 9b) but differs significantly from that of TB10.4 (Fig. 9a). The spectrum also suggests an irreversible structure change for soluble TB10.4-Ag85B

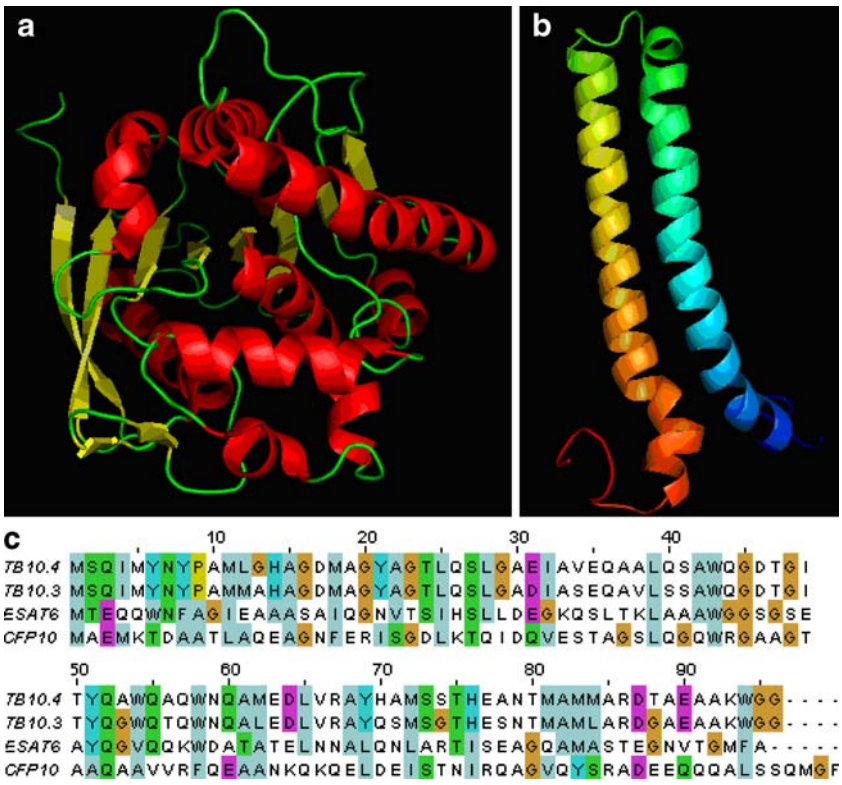

Fig. 8. Structure of Ag85B and TB10.4. **a**, structure of Ag85B (PDB accession #: 1F0N); **b**, structure of TB10.4 (simulated); **c**, multiple sequence alignment of ESAT-6 protein family members TB10.4, TB10.3, ESAT-6 and CFP-10.

(Fig. 9c, green and light blue traces as compared to the red trace). A Tm of 75.1°C was observed for soluble TB10.4-Ag85B (Fig. 9cc). In contrast, TB10.4-Ag85B purified from the inclusion body showed a reversible structure change (Fig. 9d, green trace as compared to the red trace). Moreover, no Tm was observed for this protein (Fig. 9dd). These data together suggest that TB10.4-Ag85B purified from the inclusion body with the current method does not regain the conformation adopted by its soluble counterpart.

DISCUSSION

Protein overexpression in *E. coli* frequently led to the formation of inclusion body (31,32). A high concentration of denaturant was always used to resolubilize the inclusion body, followed by protein renaturation (38). Although there are some rules to follow, successful protein renaturation is case dependent, which requires an extensive screen of buffers (39). With respect to mass production of recombinant proteins, obtaining protein from the inclusion body has several drawbacks (38). First, the use of a large amount of denaturant increases the cost of production. Second, removal of denaturant requires additional quality control. Third, it is difficult to know whether renatured proteins fully regain their conformation and function, especially for proteins that have no enzymatic activities. Despite these disadvantages, recombinant TB antigens such as Ag85B (30), TB10.4 (24), Ag85B-ESAT-6 (29) and Ag85B-TB10.4 (11) have frequently been purified from the inclusion body and formulated into TB subunit vaccine without comparing their immunogenicity to that of corresponding native antigens or soluble counterparts.

A comparison of this nature may be necessary since antigen obtained from the inclusion body may adopt a significantly different conformation (depending on renaturation) compared to its soluble counterpart or native antigens and may also mount different immune responses (40). For

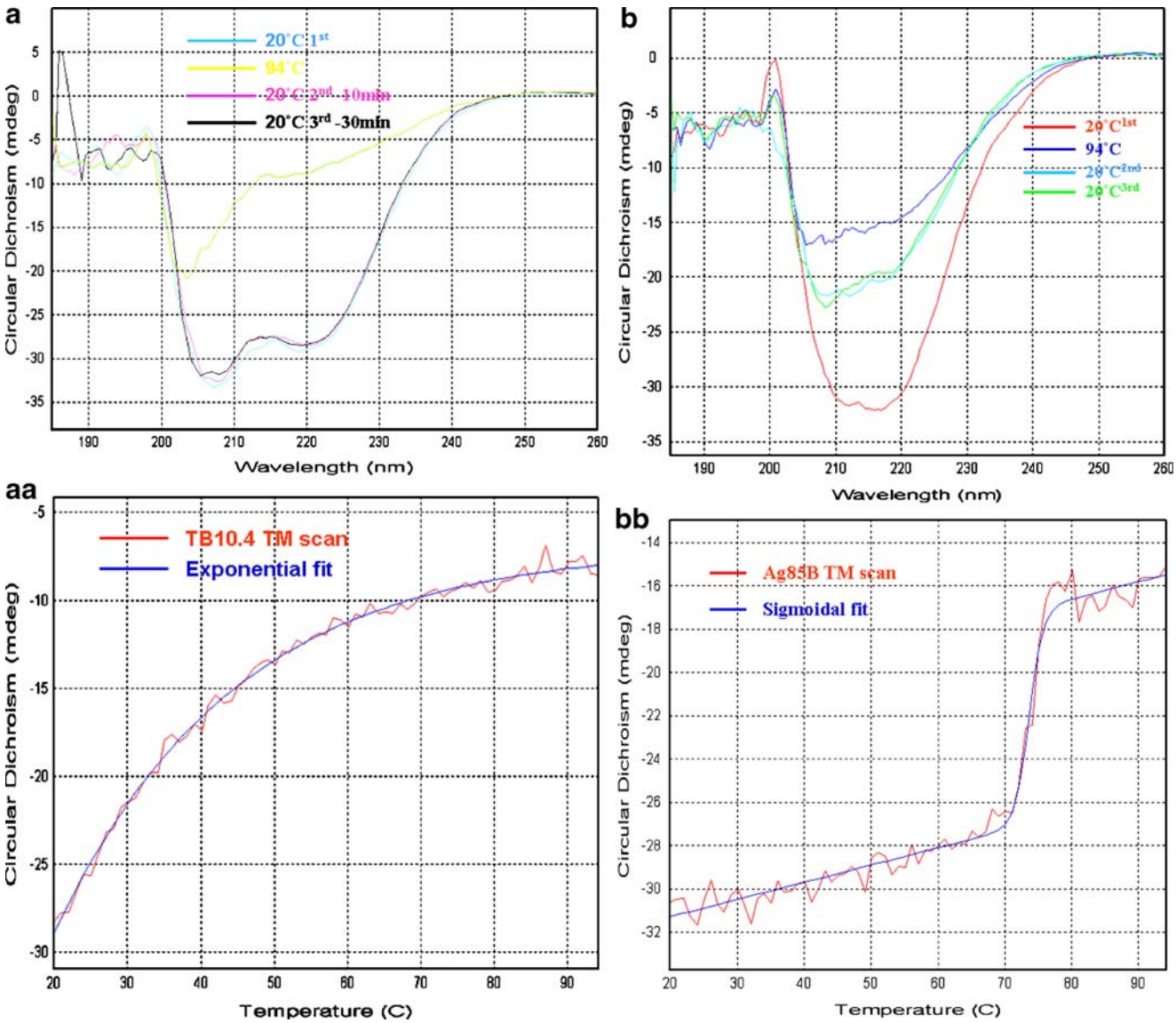

Fig. 9. Study antigen secondary structure and thermal stability by circular dichroism (CD). **a**, CD spectrum of TB10.4; **aa**, thermal stability study of TB10.4; **b**, CD spectrum of Ag85B; **bb**, thermal stability study of Ag85B; **c**, CD spectrum of soluble TB10.4-Ag85B; **cc**, thermal stability study of soluble TB10.4-Ag85B; **d**, CD spectrum of TB10.4-Ag85B purified from inclusion body; **dd**, thermal stability study of TB10.4-Ag85B purified from inclusion body.

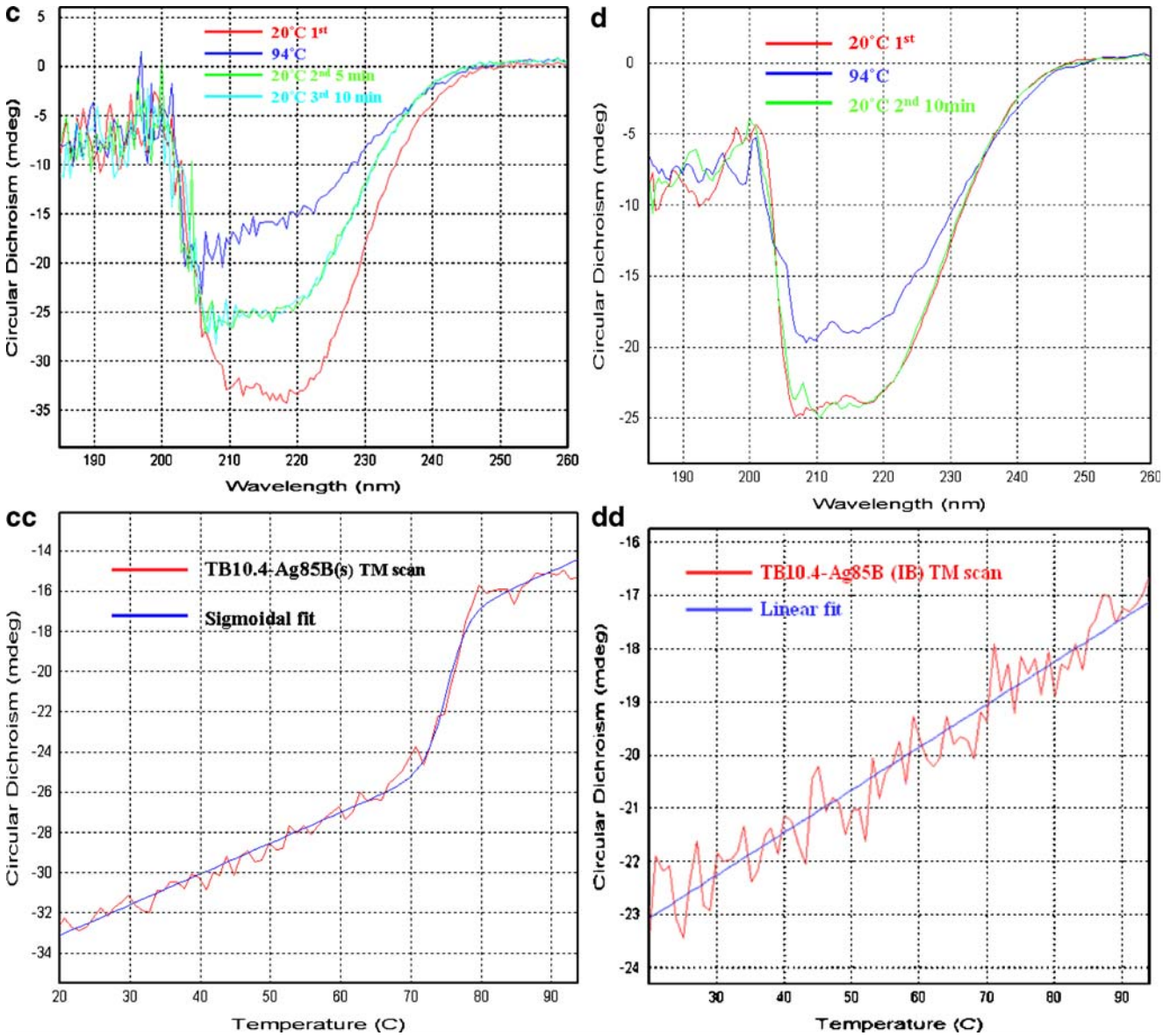

Fig. 9. (continued).

instance, it was reported that although T cells stimulated by differently folded piron protein (PrP) recognized similar immunodominant epitopes, the cytokine profiles in response to different conformers were significantly different (40). In addition, the humoral response induced by one conformer led to production of predominantly IgG1 isotype antibody; however, IgG2b was significantly produced with the other conformer immunization (40). This study indicates that both humoral and cell-mediated responses to these differently folded conformers of the same protein are quite different. This may also hold true for TB antigen-induced immune response. Therefore, it is highly favored to purify recombinant antigens from the soluble fraction, standing the best chance to fold correctly.

One possibility for inclusion body formation is that protein disulfide bonds are mismatched (38). However, this is not the case for TB10.4, since there is no cysteine residue in its primary sequence. Another reason could be that recombinant proteins are treated as exogenous when expressed in *E. coli*, whose folding machinery may not be suited to certain exogenous proteins (36). Not surprisingly, the N-terminal fusion of thioredoxin greatly improved the solubility of Trx-TB10.4, possibly because thioredoxin is an endogenous bacteria protein and its first appearance after translation can prime the bacterial folding machinery (36). It is also possible that overexpression of thioredoxin or its fusions can alter the redox environment of *E. coli* cytoplasm, creating a different folding environment (36). However, fusion of thioredoxin to the N-terminal of Ag85B-TB10.4 only slightly increased the solubility of Trx-Ag85B-TB10.4 as compared to His-Ag85B-TB10.4. In contrast, the solubility of Trx-TB10.4-Ag85B was increased by at least ten-folds as compared to Trx-Ag85B-TB10.4. These observations can be explained by two possibilities. First, the order of the fusion protein may be involved in solubility enhancement. As suggested by the terminal structure of Ag85B (Fig. 8a), seven residues were out of the secondary structure at the N-terminal,

while only three such residues exist at the C-terminal. TB10.4, however, has the same number of such residues at each terminal (Fig. 8b). These residues may serve as flexible linkers for its fusion partner. Therefore, recombinant antigen designed in the Trx-TB10.4-Ag85B direction may have a longer flexible linker as compared to Trx-Ag85B-TB10.4 between the two fusion moieties. Shorter linker in the latter design may hamper the folding of the fusion antigen. Secondly, the solubilization effect of thioredoxin on TB10.4 could be greatly diluted or compromised by the long spacer Ag85B (285 AAs) in the Trx-Ag85B-TB10.4 design.

The structure of TB10.4 lends some insights into its oligomerization. This structure may result in an extensive exposure of hydrophobic residues to the aqueous environment, thus increasing Gibbs free energy. Protein oligomerization may reduce the exposure of hydrophobic residues, thus minimizing Gibbs free energy and maximizing entropy (41). Oligomerization was also reported for CFP-10 and ESAT-6 (formation of a heterodimer), another two members in ESAT-6 family (23).

For some proteins, aggregation occurs near the isoelectric point (pI), since their surface charges are neutralized at this pH. Trx-TB10.4 and TB10.4 belong to this class of protein. It should be noticed that further decrease of pH to 3 does not lead to detectable Trx-TB10.4 aggregation, which can be explained by the fact that proteins are recharged below pI and ionic exclusion may outweigh hydrophobic interaction. However, it is still unknown whether Trx-TB10.4 possesses the same conformation at this low pH as in physiological conditions. Ag85B, which has a predicted pI of 5.24, on the other hand, does not aggregate at the testing pH range (data not shown). There are two possible explanations for this observation. First, the globular structure of Ag85B renders this protein highly resistant to pH change. Second, the actual pI for Ag85B may be significantly different from the predicted. The pI prediction by ProtParam is based on protein primary sequence, which does not take the tertiary structure into account. Some amino acids contributing to pI may hide inside the core of Ag85B and have limited or no access to the aqueous environment.

Circular dichroism (CD) is a useful tool to study protein secondary structure (42). Ag85B and soluble TB10.4-Ag85B have similar CD spectrum and a similar pattern of thermal stability. The structural characteristics for these two proteins are 1) the presence of a clear melting temperature and 2) irreversible structure change. It should be noted that the slope of the sigmoidal fit is steeper for soluble TB10.4-Ag85B than for Ag85B, which could be explained by the contribution of TB10.4 in the fusion protein. TB10.4 and TB10.4-Ag85B purified from the inclusion body, on the contrary, underwent a reversible structure change while lacking a clear melting temperature. Protein structure may explain the different behaviors in the CD experiments. Ag85B, which has a globular structure, is resistant to the temperature increase to a certain extent. At the melting temperature, the intramolecular forces are not strong enough to hold the tertiary structure; thus, a dramatic loss of CD signal occurs. Since the loss of conformation is so dramatic and fast, Ag85B may not be able to recover all intramolecular interactions correctly when cooled. In contrast, structure loss of TB10.4 took place gradually all the way with temperature increase. This may explain the reversible structure change when TB10.4 was cooled. Although soluble, TB10.4-Ag85B purified from the inclusion body does not regain the confirmation adopted by its counterpart purified from the soluble fraction. It may adopt an intermediate conformation. Since the main purpose of this study is to purify large quantities of soluble antigens, no further effort was made to optimize the renaturation condition for TB10.4-Ag85B. This could be an interesting topic for future study.

CONCLUSION

In this study, TB10.4 and TB10.4-Ag85B were expressed in *E. coli* and purified to homogeneity in great quantities. In addition, TB10.4-Ag85B is a complete new fusion molecule designed in our lab representing a promising antigen candidate for TB subunit vaccine. The rational design of the expression constructs dramatically increased the solubility and yield of the recombinant antigens leading to feasible mass production of these two antigens. CD experiments showed a significant conformation difference between TB10.4-Ag85B purified from the inclusion body and its soluble counterpart. The pH and thermal stability data provide invaluable information that will guide further formulation development based on these two antigens.

ACKNOWLEDGEMENTS

The authors greatly appreciate the gift of *E. coli JM109DE* strain carrying Ag85B gene by Dr. Douglas Kernodle in Vanderbilt University. The authors are also thankful to Dr. Miriam Braunstein and Mrs. Jessica McCann for providing H37Rv genome DNA.

REFERENCES

1. Flynn JL, Chan J. Immunology of tuberculosis. Annu Rev Immunol. 2001;19:93–129.
2. Dunlap NE, Briles DE. Immunology of tuberculosis. Med Clin North Am. 1993;77:1235–51.
3. Flynn JL, Chan J. Tuberculosis: latency and reactivation. Infect Immun. 2001;69:4195–201.
4. Brimnes N. BCG vaccination and WHO's global strategy for tuberculosis control 1948–1983. Soc Sci Med. 2008;67:863–73.
5. Colditz GA, Brewer TF, Berkey CS, Wilson ME, Burdick E, Fineberg HV, *et al*. Efficacy of BCG vaccine in the prevention of tuberculosis: meta-analysis of the published literature. J Am Med Assoc. 1994;271:698–702.
6. Fine PE. Variation in protection by BCG: implications of and for heterologous immunity. Lancet. 1995;346:1339–45.
7. Sterne JA, Rodrigues LC, Guedes IN. Does the efficacy of BCG decline with time since vaccination? Int J Tuberc Lung Dis. 1998;2:200–7.
8. Rodrigues LC, Pereira SM, Cunha SS, Genser B, Ichihara MY, de Brito SC, *et al*. Effect of BCG revaccination on incidence of tuberculosis in school-aged children in Brazil: the BCG-REVAC cluster-randomised trial. Lancet. 2005;366:1290–5.
9. Mittal SK, Aggarwal V, Rastogi A, Saini N. Does B.C.G. vaccination prevent or postpone the occurrence of tuberculosis meningitis? Indian J Pediatr. 1996;63:659–64.
10. Colditz GA, Berkey CS, Mosteller F, Brewer TF, Wilson ME, Burdick E, *et al*. The efficacy of bacillus Calmette-Guerin

vaccination of newborns and infants in the prevention of tuberculosis: metaanalyses of the published literature. Pediatrics. 1995;96:29.
11. Dietrich J, Aagaard C, Leah R, Olsen AW, Stryhn A, Doherty TM, *et al*. Exchanging ESAT6 with TB10.4 in an Ag85B fusion molecule-based tuberculosis subunit vaccine: efficient protection and ESAT6-based sensitive monitoring of vaccine efficacy. J Immunol. 2005;174:6332–9.
12. Horwitz MA, Harth G. A new vaccine against tuberculosis affords greater survival after challenge than the current vaccine in the guinea pig model of pulmonary tuberculosis. Infect Immun. 2003;71:1672–9.
13. Horwitz MA, Harth G, Dillon BJ, Maslesa-Galic S. Recombinant bacillus calmette-guerin (BCG) vaccines expressing the Mycobacterium tuberculosis 30-kDa major secretory protein induce greater protective immunity against tuberculosis than conventional BCG vaccines in a highly susceptible animal model. Proc Natl Acad Sci USA. 2000;97:13853–8.
14. Soto CY, Menendez MC, Perez E, Samper S, Gomez AB, Garcia MJ, *et al*. IS6110 mediates increased transcription of the phoP virulence gene in a multidrug-resistant clinical isolate responsible for tuberculosis outbreaks. J Clin Microbiol. 2004;42:212–9.
15. Perez E, Samper S, Bordas Y, Guilhot C, Gicquel B, Martin C. An essential role for phoP in Mycobacterium tuberculosis virulence. Mol Microbiol. 2001;41:179–87.
16. Havenga M, Vogels R, Zuijdgeest D, Radosevic K, Mueller S, Sieuwerts M, *et al*. Novel replication-incompetent adenoviral B-group vectors: high vector stability and yield in PER.C6 cells. J Gen Virol. 2006;87:2135–43.
17. Belisle JT, Vissa VD, Sievert T, Takayama K, Brennan PJ, Besra GS. Role of the major antigen of Mycobacterium tuberculosis in cell wall biogenesis. Science. 1997;276:1420–2.
18. Daffe M. The mycobacterial antigens 85 complex — from structure to function and beyond. Trends Microbiol. 2000;8: 438–40.
19. Wiker HG, Harboe M. The antigen 85 complex: a major secretion product of Mycobacterium tuberculosis. Microbiol Rev. 1992;56:648–61.
20. Lu D, Garcia-Contreras L, Xu D, Kurtz SL, Liu J, Braunstein M, *et al*. Poly (lactide-co-glycolide) microspheres in respirable sizes enhance an *in vitro* T cell response to recombinant Mycobacterium tuberculosis antigen 85B. Pharm Res. 2007;24:1834–43.
21. Olsen AW, van Pinxteren LA, Okkels LM, Rasmussen PB, Andersen P. Protection of mice with a tuberculosis subunit vaccine based on a fusion protein of antigen 85b and esat-6. Infect Immun. 2001;69:2773.
22. Skjot RL, Oettinger T, Rosenkrands I, Ravn P, Brock I, Jacobsen S, *et al*. Comparative evaluation of low-molecular-mass proteins from Mycobacterium tuberculosis identifies members of the ESAT-6 family as immunodominant T-cell antigens. Infect Immun. 2000;68:214–20.
23. Renshaw PS, Lightbody KL, Veverka V, Muskett FW, Kelly G, Frenkiel TA, *et al*. Structure and function of the complex formed by the tuberculosis virulence factors CFP-10 and ESAT-6. Embo J. 2005;24:2491–8.
24. Skjot RL, Brock I, Arend SM, Munk ME, Theisen M, Ottenhoff TH, *et al*. Epitope mapping of the immunodominant antigen TB10.4 and the two homologous proteins TB10.3 and TB12.9, which constitute a subfamily of the esat-6 gene family. Infect Immun. 2002;70:5446–53.
25. Bae K, Choi J, Jang Y, Ahn S, Hur B. Innovative vaccine production technologies: the evolution and value of vaccine production technologies. Arch Pharm Res. 2009;32:465–80.
26. Skeiky YA, Sadoff JC. Advances in tuberculosis vaccine strategies. Nat Rev Microbiol. 2006;4:469–76.
27. Chawla A, Midha S, Bhatnagar R. Efficacy of recombinant anthrax vaccine against Bacillus anthracis aerosol spore challenge: preclinical evaluation in rabbits and Rhesus monkeys. Biotechnol J. 2009;4:391–9.
28. Song L, Nakaar V, Kavita U, Tussey L. Efficacious Recombinant Influenza Vaccines Produced by High Yield Bacterial Expression: A Solution to Global Pandemic and Seasonal Needs. PLoS ONE. 2008;3:e2257.
29. Shi CH, Fan XL, Xu ZK, Li Y, Bai YL, Xue Y. Mycobacterium tuberculosis secreting protein Ag85B-ESAT6 fused expression and purification. Zhonghua Jie He He Hu Xi Za Zhi. 2004;27:89–92.
30. Lakey DL, Voladri RK, Edwards KM, Hager C, Samten B, Wallis RS, *et al*. Enhanced production of recombinant Mycobacterium tuberculosis antigens in Escherichia coli by replacement of low-usage codons. Infect Immun. 2000;68:233–8.
31. Baneyx F, Mujacic M. Recombinant protein folding and misfolding in Escherichia coli. Nat Biotechnol. 2004;22:1399–408.
32. Mitraki A, King J. Protein Folding Intermediates and Inclusion Body Formation. Nat Biotechnol. 1989;7:690–7.
33. Adler S, Modrich P. T7-induced DNA polymerase. Requirement for thioredoxin sulfhydryl groups. J Biol Chem. 1983;258:6956–62.
34. Mukherjee A, Martin SG. The thioredoxin system: a key target in tumour and endothelial cells. Br J Radiol. 81 Spec No 1:S57-68 (2008).
35. Hall A, Parsonage D, Horita DA, Karplus PA, Poole LB, Barbar EJ. Redox dependent dynamics of a dual thioredoxin-fold protein: evolution of specialized folds. Biochemistry. 2009.
36. LaVallie ER, DiBlasio EA, Kovacic S, Grant KL, Schendel PF, McCoy JM. A thioredoxin gene fusion expression system that circumvents inclusion body formation in the E. coli cytoplasm. Biotechnology (N Y). 1993;11:187–93.
37. Bayer ME. Areas of adhesion between wall and membrane of Escherichia coli. J Gen Microbiol. 1968;53:395–404.
38. Clark EDB. Protein refolding for industrial processes. Curr Opin Biotechnol. 2001;12:202–7.
39. Khan MA, Sadaf S, Sajjad M, Akhtar MW. Production enhancement and refolding of caprine growth hormone expressed in Escherichia coli. Protein Expr Purif. 2009.
40. Khalili-Shirazi A, Quaratino S, Londei M, Summers L, Collinge J. Protein conformation significantly influences immune responses to prion protein. J Immunol. 2005;174:3256–63.
41. Sinha S, Surolia A. Oligomerization endows enormous stability to soybean agglutinin: a comparison of the stability of monomer and tetramer of soybean agglutinin. Biophys J. 2005;88:4243–51.
42. Jiang G, Joshi SB, Peek LJ, Brandau DT, Huang J, Ferriter MS, *et al*. Anthrax vaccine powder formulations for nasal mucosal delivery. J Pharm Sci. 2006;95:80–96.